An array of layers in silicon sulfides: Chainlike and monolayer

T. Alonso-Lanza,[1,*] A. Ayuela,[1] and F. Aguilera-Granja[1,2]

[1]*Centro de Física de Materiales CFM-MPC CSIC-UPV/EHU, Donostia International Physics Center (DIPC), Departamento de Física de Materiales, Facultad de Químicas, UPV-EHU, 20018 San Sebastián, Spain*

[2]*Instituto de Física, Universidad Autónoma de San Luis de Potosí, 78000 San Luis Potosí, San Luis Potosí, México*

(Received 9 August 2016; revised manuscript received 12 November 2016; published 29 December 2016)

While much is known about isoelectronic materials related to carbon nanostructures, such as boron-nitride layers and nanotubes, rather less is known about equivalent silicon-based materials. Following the recent discovery of phosphorene, here we discuss isoelectronic silicon-monosulfide monolayers. We describe a set of anisotropic structures that clearly have a high stability with respect to previously reported silicon-monosulfide monolayers. The source of the layer anisotropy is related to the presence of Si-S double chains linked by some Si-Si covalent bonds together with a remarkable *spd* hybridization on Si. The increased stability is related to silicon forming four bonds, including an additional double-bond-like Si-Si bond. The involvement of *d* orbitals brings more variety to silicon-sulfide-based nanostructures that are isoelectronic to phosphorene, which could be relevant for future applications, adding extra degrees of freedom.

DOI: 10.1103/PhysRevB.94.245441

I. INTRODUCTION

The isolation of a single layer of carbon atoms in 2004 [1] opened up a new and exciting field in science related to the study and characterization of monolayers, which is still a growing field today. The impressive electronic, optical, and mechanical properties of graphene [2–7] were a key motivation in the search for new monolayers, which has the aim of discovering nanomaterials that do not have the drawbacks that graphene has in some applications, such as the absence of a band gap; alternatively, some new and unexpected properties caused by bidimensionality may be possible. The growing interest in graphene is currently driving the development of experimental techniques needed to characterize single-layer materials with sufficient accuracy [8–10]. This improvement, together with the possibility of exfoliating weakly bound layered materials, explains the proliferation of interest in new two-dimensional layers. Among the isoelectronic compounds of graphene are boron nitride and silicene. Boron-nitride nanotubes were synthesized [11] within the carbon row of the periodic table, and hexagonal boron-nitride layers were later exfoliated from bulk in the most stable phase which is built from weakly bound monolayers [12]. Lower down in the same periodic-table group, silicene was synthesized experimentally some years ago [13–15]. Silicene has some important differences from graphene, including a buckled structure due to pseudo-Jahn-Teller distortion [16,17], higher reactivity, and a more easily tunable gap by surface adsorption [18,19]. All these silicon-type properties stem for the sp^3 hybridization and the double-bond rule [20–22], which state that double bonds are not formed for elements in the third period such as silicon. Other group-IV structures similar to graphene and graphane have been proposed [23]. Nevertheless, the field has broadened to systems noticeably different from graphene. Our interest lies in the search for isoelectronic compounds related to other recent synthesized monolayers, but which still have silicon with its special properties as a principal ingredient.

A new impetus has recently come from the study of single layers of black phosphorus [24,25], termed phosphorene in analogy with graphene and having desirable characteristics for electronics, including high carrier mobility, anisotropic electronic properties, and a band gap that depends on thickness [26]. Despite some drawbacks in terms of fast degradation on contact with air [27,28], phosphorene shows promise for applications such as field-effect transistors [29,30]. For this reason, the investigation of isoelectronic compounds of phosphorene is currently of great interest. The same line of enquiry has led to the proposal of isoelectronic monolayers composed of group-V elements made either of single elements, such as arsenic and antimony monolayers known as arsenene and antimonene [31,32], or mixed together as AsP and SbP [33]. Furthermore, the significance of boron nitride (with respect to graphene) shows that it is logical to consider compounds of groups IV–VI, also called group-IV monochalcogenides [34–36], which are also isoelectronic to phosphorene as well as being semiconductors with band gaps larger than those in the bulk phase [37]. Among these, our attention was drawn particularly to silicon monosulfide. Monolayers of this material have been reported to display two structures close together in energy, with the more stable of these being similar to buckled graphene and the other slightly less stable being similar to phosphorene [38], which has been recently proposed as an anode material in Li-ion batteries [39]. Although both forms contain silicon atoms bonded to three different sulfur atoms, silicon compounds can present higher coordination, sometimes even being pentacoordinated [40,41, and references therein]. We must therefore allow for the greater coordination of silicon atoms within silicon-monosulfide two-dimensional layers when considering the range of possible forms.

In this work, we present an anisotropic γ structure for the silicon monolayer that greatly improves stability compared with previous reports of two-dimensional layers. We begin by considering the geometry of the SiS phase, which contains silicon-silicon bonds while each silicon atom also remains bonded to three sulfur atoms. In our simulations, we found that this anisotropic and more stable γ layer maintains its structural integrity at room temperature. We analyzed the bonding and the hybridization of the sulfur and silicon atoms

*Corresponding author: tomas_alonso001@ehu.eus

and found that the silicon-silicon bond seems to behave like a double bond, in violation of the double-bond rule. More importantly, the coordination shown by the silicon atoms is strongly influenced by *spd* hybridization. This finding paves the way using large cells for the search of a whole array of two-dimensional structures that are both stable and highly anisotropic, all of which could be of interest, for instance, in the patterning of nanostructures with specific properties on various substrates.

II. COMPUTATIONAL DETAILS

We performed calculations on silicon-sulfide nanostructures using the SIESTA (Spanish Initiative for Electronic Simulations with Thousands of Atoms) method, making reference to density functional theory. For the exchange and correlation potentials, the Perdew-Burke-Ernzenhof form of the generalized gradient approximation (GGA) [42] is well suited to the study of these kinds of covalent nanolayers in combination with the description of atomic cores by nonlocal norm-conserving Troullier-Martins [43] pseudopotentials factorized in the Kleynman-Bylander form. A double-ζ plus polarization orbitals basis set for valence electrons was used. The same computational parameters were used in all the calculations, namely an electronic temperature of 25 meV and a mesh cutoff of 250 Ry. We sample the Brillouin zone using a k-grid cutoff of 25 Å. All cells were assigned large vectors (24.5 Å) in the direction perpendicular to the monolayers in order to avoid monolayer-monolayer interactions. We fully relaxed both the atoms and the unit cell until forces are well converged below 0.006 eV/Å. Given the importance of stability, we also carried out molecular dynamics simulations using the Nose thermostat, and we used a Nose mass of 10.0 Ry f^2 and a time step of 1 fs [44–46]. We have chosen 3000 as the final time step, and the relaxation time to reach the target temperature was 2500 fs. We checked the validity of our results by repeating key calculations using the VASP code, which uses the projected augmented wave (PAW) method [47,48].

III. RESULTS AND DISCUSSION

A. Monolayers

1. Anisotropy in highly stable structures

Figure 1 shows three different monolayer arrangements. We obtained a monolayer labeled γ which improves the binding energy per atom by 88 meV with respect to the recently proposed α and β structures [38]. We note that this SiS phase is more stable than the other two forms according to two different codes: the VASP values are shown in parentheses in Fig. 1. The previously reported α and β monolayers were obtained using a restriction to three coordinated elements in either isotropic hexagonal or rectangular (close to square) structures. Our results are in full agreement with this previous study, although we found β to be more stable than α, by 4 meV instead of the reported 12 meV, because the distances for the α monolayer are slightly different. More importantly, we found the γ phase for the SiS monolayer because the unit cell was assumed rhombohedral, and it is crucial that it contains two silicon and two sulfur atoms. Silicon-monosulfide monolayers therefore present a more stable phase when larger cells are allowed. We checked the stability of the γ monolayer using a 3×3 supercell with 36 atoms. We found that the γ monolayer structure is well preserved.

Although the structure of black phosphorous is known to have some underlying anisotropy, this is clearly revealed in the γ low-lying stable layer when larger cells are allowed. Figure 1 shows alternating parallel rows of rippled hexagons and squares along the y direction. Matching these two patterns, silicon atoms adopt a fourfold coordination, where they bind to three sulfur atoms in the squares and, more interestingly, form Si-Si dimers ribbing the hexagons at the sides in a stairlike fashion. Silicon establishing four bonds is related to the increased stability; this is in agreement with Ref. [49] with the silicon atom preferring to have four bonds rather than three.

We then applied molecular dynamics using the Nose thermostat to study the stability of the γ monolayers. We used a supercell of 36 atoms to carry out the simulation. Figure 2(a) shows the energy on each step of the Nose thermostat at 300 K. The energy fluctuates slightly accordingly to the small

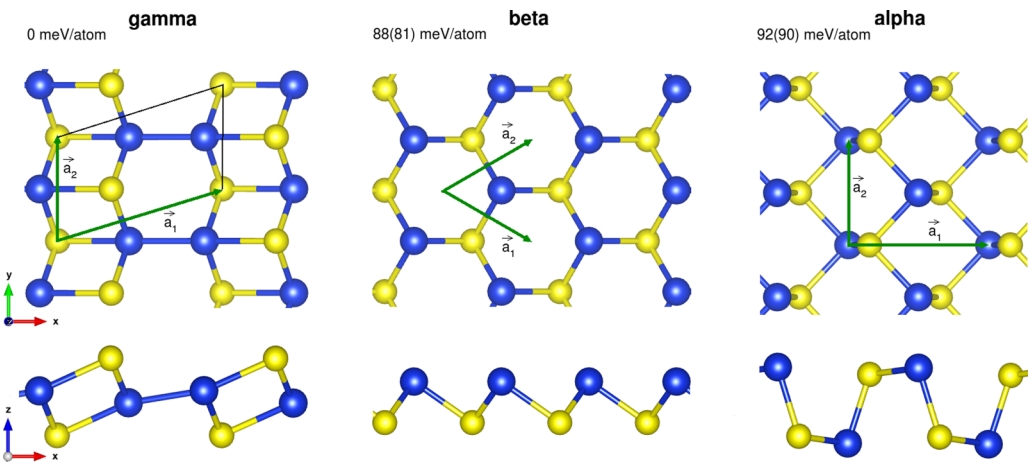

FIG. 1. Geometries of three silicon-monosulfide monolayers in order of increasing energy. Energies in parentheses correspond to test results obtained using the VASP code. The unit cell employed for the electronic analysis is shown in each case. Silicon (sulfur) atoms are denoted by blue (yellow) spheres; this color code is used throughout. The γ layer is the most stable and anisotropic of the three forms.

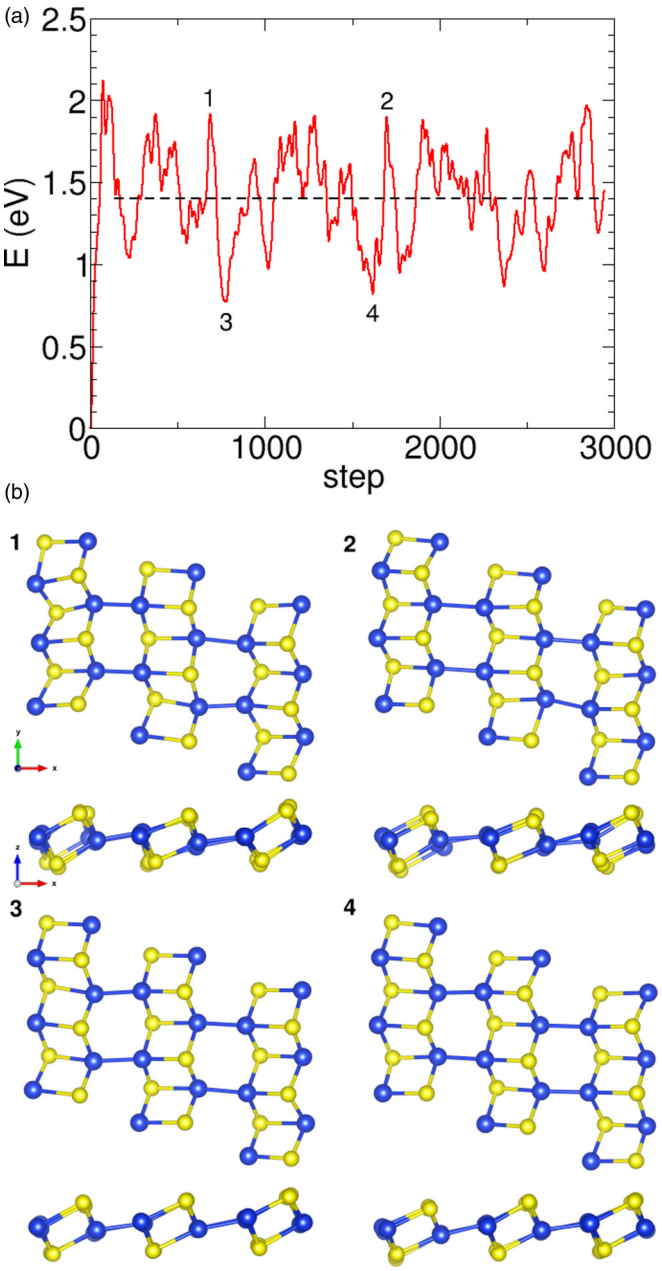

FIG. 2. (a) Energy vs time step for the γ silicon-monosulfide monolayer in a Nose thermostat at 300 K; (b) snapshots at the four steps marked up in (a).

displacements of the atoms with respect to their equilibrium positions, which can be seen in Fig. 2(b). Attending to our simulations, we can affirm that the structure is stable up to room temperature. In the Supplemental Material [50], there are two (shown in top and side views) animations that collect the movements of the atoms during the simulations, showing that they just oscillate around their original position. On the other hand, we double checked the stability by computing the phonon dispersion of the γ silicon-monosulfide monolayer as shown in Fig. 3.

Regarding a possible future synthesis, we propose chemical vapor deposition (CVD) as the experimental technique, using an appropriate compound of silicon and sulfur powders as precursor materials. Both would react in a furnace at high temperatures, leading to the formation of the SiS monolayer over a substrate still to be determined, which could be graphene. Control of rates, substrate treatments, and election of precursor materials and their quantities could help to obtain different SiS phases. However, details of the procedures are beyond the scope of the present work. We encourage experimental groups to synthesize silicon-monosulfide monolayers.

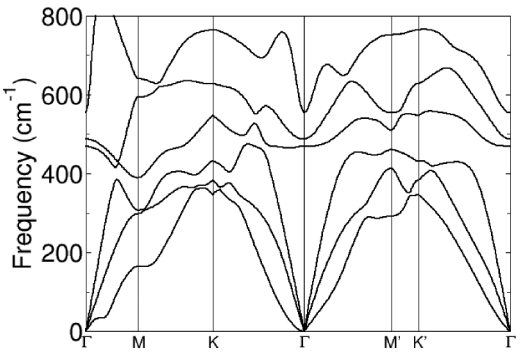

FIG. 3. Phonon dispersion of γ silicon-monosulfide monolayer.

2. *spd hybridization in Si bonds*

We now look in detail at the bonding parameters with the aim of clarifying the mechanism that explains the stability order. First, we note that β and α monolayers each have a silicon bonded to three sulfur atoms, with three distances of 2.37 Å for the isotropic β, and two of 2.37 Å and one of 2.39 Å for the α. The analysis is completed by measuring the angles between the established bonds, which are 90° for β and one of 93° and two of 97° for α. Note that the local environment of the atom is very similar for α and β structures, which explains the similar stability, as reported for phosphorene phases [51]. However, the silicon atoms in the γ monolayer present four bonds instead of three, which constitutes a significant difference with respect to the structures described above following a trend previously proposed [49]. Three bonds are still made with sulfur atoms of about 2.31 Å, and the extra one links two silicon atoms separated by 2.50 Å. The angles between bonds are key for looking at hybridizations. There are two S-Si-S angles of 92° and one of 94°, and there are two Si-Si-S angles of 99° and one of 164°. The neighboring silicon atoms form right angles in almost all directions, enforcing a hybridization different from the sp^3 hybridization found for silicon bulk [52]. This symmetry requires the participation of d orbitals in a *spd* hybridization. The involvement of d electrons on Si seems key to explain the bond in the γ SiS monolayers.

In order to assess the hybridization in more detail, we consider the electronic structure of the γ layer. The density of states (DOS) projected for the silicon and sulfur orbitals are shown in Fig. 4(a). The total DOS below the Fermi energy is composed of four distinct zones separated by small gaps in energy. The rectangles in Fig. 4 enclose the four different zones in terms of energy and we detail the orbital contribution further. Notice that the contribution of sulfur is larger than that of silicon for almost all zones because of the high number of valence electrons. More relevant is the fact that in zone 4, the peak close to the Fermi energy has a preeminent contribution from silicon. The s and p

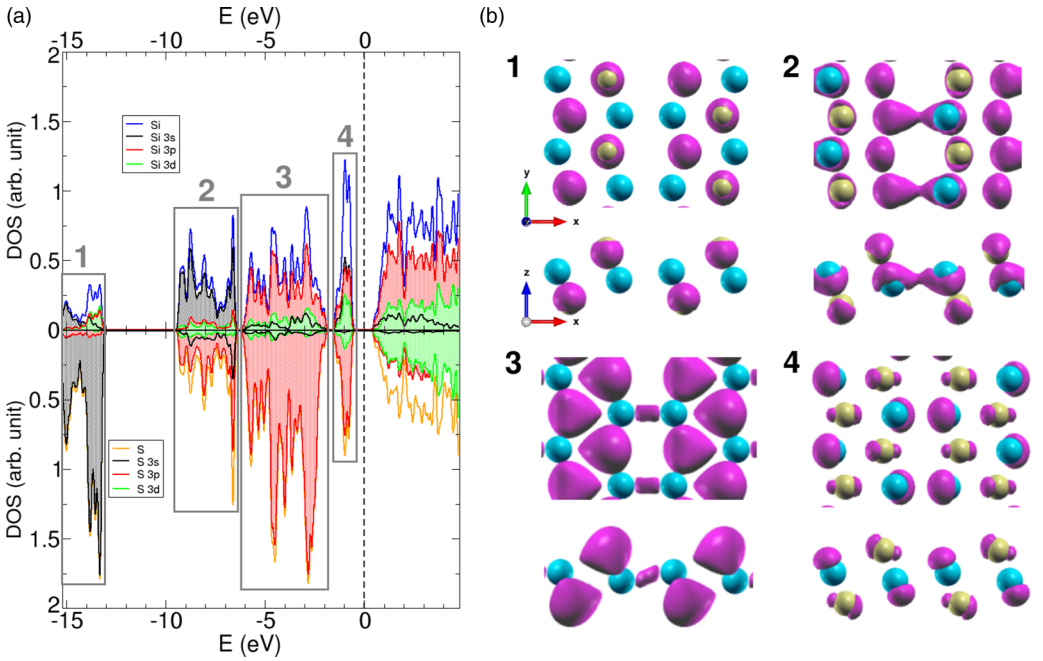

FIG. 4. Electronic structure of γ monolayer. (a) Projected density of states. The four zones 1–4 highlighted within the rectangles are separated by small gaps. (b) Local density of states in energy zones 1–4 shown by lobules. Zones 2 and 3 have a component in the Si-Si bond. Zone 4 is p on sulfur and a dangling bond on Si, with a large spd hybridization.

contribution of silicon in this zone 4 is almost equal, and the d contribution surprisingly amounts to half the s and p contributions, a fact that indicates spd hybridization. Notice that the d contribution is negligible for the α and β phases, as shown in the Supplemental Material [50].

At deeper energies, we find consecutively two zones, 3 and 2, that are mainly contributed by p and s Si orbitals, respectively. Looking at the sulfur orbitals, we find s states deep in energy in zone 1, but scarcely hybridized with p orbitals in other zones, which constitutes almost all of the contribution of sulfur at higher energies, now with a much smaller d part than at the highest occupied energy. We illustrate the energy zones in space using the localized density of states (LDOS) in Fig. 4(b). We find that the silicon-silicon bond comes mainly from σ- and π-like states in zones 2 and 3, respectively, lying lower than the Fermi energy. This seems to be evidence of a double bond between two silicon atoms, adding to the body of few known cases where the double-bond rule is not satisfied. As previously commented, the role of this bond is to enhance stability in the SiS layers, which clarifies its importance.

It is noteworthy that just below the Fermi energy, in zone 4, the LDOS shape is p-like over sulfur atoms and has lobules on silicon stemming from the hybridization of spd electrons, in agreement with the above results. These lobules on silicon represent something like a dangling bond. Even though both zones 3 and 4 have p contributions, we note by looking at the side views of zones 3 and 4 that they are largely orthogonal to each other.

3. *Anisotropy in band structures*

We next comment in detail on the implications of the anisotropy on the electronic band structures, as shown in Fig. 5 for the three different monolayers. The band structures we obtained for α and β layers faithfully reproduce those presented previously, and the band gaps are 1.5 and 2.3 eV, respectively [38]. A common feature among all of them is the presence of an indirect band gap. The band gap for γ, the most stable among the thinnest nanostructures of silicon monosulfide, decreases to 1.13 eV, the smaller value of the three monolayers, so the assumed correlation between the gap and the stability does not apply [54]. Note that the well-known underestimation of the band gap by the generalized gradient approximation ensures the insulating character of the system. It should be noted that the presence of an isolated valence band close to the Fermi energy for the γ layer is a feature that distinguishes it from the α and β ones. This band is localized and it also presents a gap with respect to lower bands. The origin of this band was clarified above as being due to p_z-like sulfur orbitals and spd Si lobes. Furthermore, for the γ monolayer, the rhombohedral unit cell implies a distorted hexagonal Brillouin zone. The band is anisotropic in the plane and the valence-conductance distance is lower around the M-K point, where there is a strong y component along the Si dimers. They seem crucial not only in terms of stability, but also for the peculiar anisotropic properties in holes or electrons, which could be important for future applications of SiS monolayers in the design of possible conductance devices.

B. More SiS structures

In addition to the findings outline above, we found other anisotropic structures with chainlike geometries where the number of atoms per cell is much greater than in the γ, α, and β structures described above. As input structures, we generated a great variety of bipartite lattices with different symmetries such as square, rectangular, and hexagonal, giving

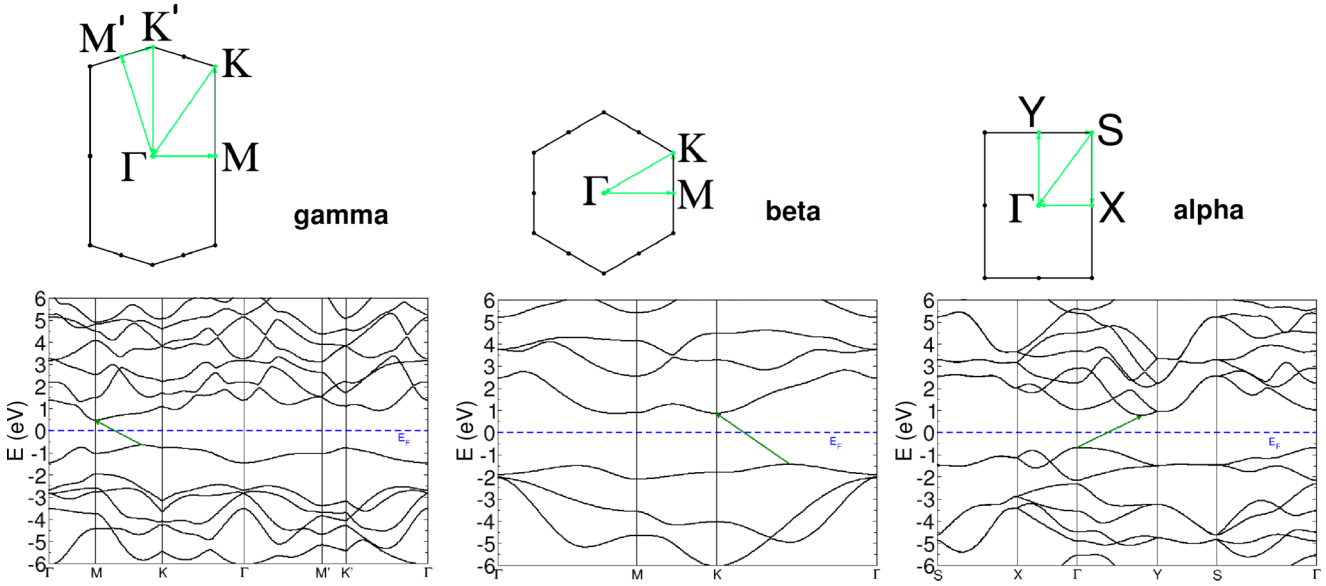

FIG. 5. Band structures of three silicon-monosulfide monolayers together with the path followed in the reciprocal space for each case.

the possibility of steps of different heights. All these initial models were then optimized by relaxing positions and cell lattice vectors. In Fig. 6, we display two of the most stable structures we have found thus far. These structures present a long-range spatial order and are more stable than the regular ones given above: one of them is even preferred to the γ monolayer by 83 meV/atom. In line with the findings for the γ monolayer, the structures present the same pattern: more or less complicated chains of Si-S repeated and linked by silicon-silicon covalent bonds between adjacent chains. The distance between these Si-Si bonds is around 2.4 Å, denoting strong bonding as for the γ monolayer.

We found other metastable structures such as those shown in Fig. 6 competing in energy with the γ monolayer, established as the zero of energy. The cross sections of Fig. 6 show that those structures are typically thicker. The number of atoms per surface unit is increased, which could add to the enhancement of stability with respect to the monolayers, with lower densities with thicknesses of barely two atoms. However, larger densities do not always imply larger stability [53]. On the other hand, sulfur establishes only two bonds to fulfill the octet rule [49], which is a source of extra stability. Another difference is the increase in the number of silicon atoms bound together, with Si linear chains up to four atoms, which seems to percolate through SiS layers. The presence of silicon-silicon bonds within a chain lowers the coordination of the sulfur atoms in order to maintain the stoichiometry of SiS, which produces holes in the structure favoring the wire in the long-range structure. The number of different structures suggests the richness of the different configurations that may occur due to different hybridizations in the electronic structures, clearly different from graphene, particularly in the case of those elements closely isoelectronic to the phosphorene group and in the same row of the periodic table. Recently, we discovered that other highly stable structures composed of SiS were reported by Yang *et al.* [49]. They propose a ground-state structure similar to the structure labeled as A in Fig. 6, which we found as the most stable. Silicon atoms establish four bonds and sulfur atoms have two bonds, a bonding pattern which agrees with the idea reported by these authors [49]. The rise of stability is explained due to the number of bonds established by silicon and sulfur, as commented above. Structure stability depends not only on thickness. Other issues, such as the kind of bonds established by silicon and sulfur, can also be relevant. In particular, thicker structures allow environments for the atoms with standard orbital hybridizations, while very thin structures could have other optional hybridizations. We separated those structures in a different section because they are thicker than the γ monolayer. For the sake of clarity, we present the five stable structures for SiS with their thicknesses in Fig. 7. The *Pma*2 structure is thicker than the α and γ phases, which are equally thick. The β phase is thinner than the α phase; however, it shows a similar stability due to having a similar local environment [51]. *Silicene sulfide*

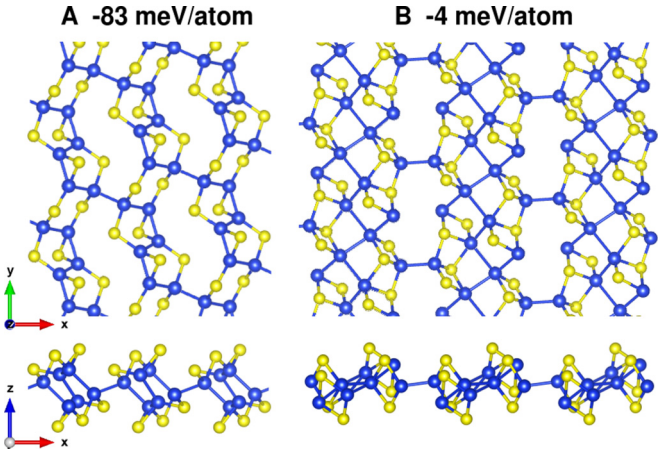

FIG. 6. Examples of metastable monosulfide chainlike structures linked by Si dimer, obtained with large cells. The reference for energies is referred to the γ monolayer from Fig. 1. Note that Si atoms form larger chains, percolating through the SiS layer. An additional two different structures are shown in the Supplemental Material [50].

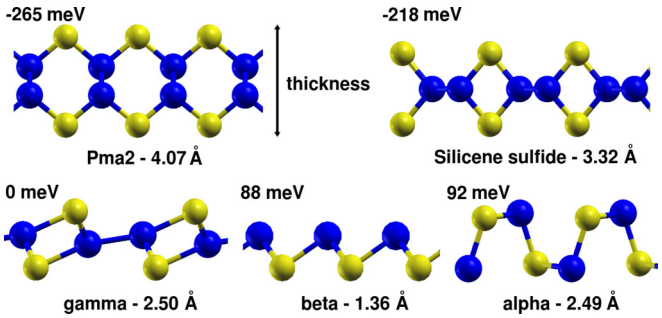

FIG. 7. Side views of five different phases already reported for silicon monosulfide including their thicknesses in angstrom units and the relative stability in meV attending to our calculations.

structure appears halfway between γ and $Pma2$, but close to $Pma2$. Therefore, among the thinnest SiS structures, the γ phase is the most stable because it includes a fourth bond for silicon. The thickest structures are more stable for SiS because they let sulfur establish only two bonds rather than three. It remains a challenge to design thinner structures, as the γ phase, following the high stable bonding scheme of four and two bonds for silicon and sulfur, respectively.

IV. SUMMARY AND CONCLUSIONS

In summary, we have presented a different silicon-monosulfide phase monolayer labeled as γ for silicon monosulfide. It has enhanced stability with respect to the α and β monolayers. Following the search for the γ layer, we also found several forming an array of silicon-monosulfide thicker layers. All of these structures present chains with a long-range spatial order and silicon-silicon bonds linking them, either more stable than the γ monolayer or competing with it. The silicon atoms participate in direct Si-Si double bond where s, p, and d orbitals hybridize, like *spd*. The extra stability for the γ monolayer and the related structures comes from the extra silicon-silicon bond, which was not present in the other silicon-monosulfide monolayers α and β, and brings forward the structure and electronic anisotropy of these layers. It seems that the anisotropy in structures and bands isoelectronic to phosphorene differs from compounds isoelectronic to graphene, and can be important for hole and electron conductance in SiS monolayers.

ACKNOWLEDGMENTS

This work has been partially supported by the Projects No. FIS2013-48286-C2-1-P and No. FIS2016-76617-P of the Spanish Ministry of Economy and Competitiveness MINECO, the Basque Government under the ETORTEK Program 2014 (nanoGUNE2014), and the University of the Basque Country (Grant No. IT-366-07). T.A.-L. acknowledges the grant of the MPC Material Physics Center - San Sebastián. F.A.-G. acknowledges the DIPC for their generous hospitality. We also want to acknowledge the DIPC computer center (T.A.L., A.A., and F.A.-G.).

[1] K. S. Novoselov, A. K. Geim, S. V. Morozov, D. Jiang, Y. Zhang, S. V. Dubonos, I. V. Grigorieva, and A. A. Firsov, Science **306**, 666 (2004).
[2] K. S. Novoselov, V. I. Fal'ko, L. Colombo, P. R. Gellert, M. G. Schwab, and K. Kim, Nature (London) **490**, 192 (2012).
[3] X. Huang, Z. Yin, S. Wu, X. Qi, Q. He, Q. Zhang, Q. Yan, F. Boey, and H. Zhang, Small **7**, 1876 (2011).
[4] A. K. Geim, Science **324**, 1530 (2009).
[5] A. H. C. Neto, F. Guinea, N. M. R. Peres, K. S. Novoselov, and A. K. Geim, Rev. Mod. Phys. **81**, 109 (2009).
[6] K. I. Bolotin, K. J. Sikes, Z. Jiang, M. Klima, G. Fudenberg, J. Hone, P. Kim, and H. L. Stormer, Solid State Commun. **146**, 351 (2008).
[7] Y. Zhang, Y.-W. Tan, H. L. Stormer, and P. Kim, Nature (London) **438**, 201 (2005).
[8] A. Hashimoto, K. Suenaga, A. Gloter, K. Urita, and S. Iijima, Nature (London) **430**, 870 (2004).
[9] Z. Liu, K. Suenaga, P. J. F. Harris, and S. Iijima, Phys. Rev. Lett. **102**, 015501 (2009).
[10] C. Jin, H. Lan, L. Peng, K. Suenaga, and S. Iijima, Phys. Rev. Lett. **102**, 205501 (2009).
[11] N. G. Chopra, R. J. Luyken, K. Cherrey, V. H. Crespi, M. L. Cohen, S. G. Louie, and A. Zettl, Science **269**, 966 (1995).
[12] A. Zunger, A. Katzir, and A. Halperin, Phys. Rev. B **13**, 5560 (1976).
[13] P. Vogt, P. De Padova, C. Quaresima, J. Avila, E. Frantzeskakis, M. C. Asensio, A. Resta, B. Ealet, and G. Le Lay, Phys. Rev. Lett. **108**, 155501 (2012).
[14] B. Lalmi, H. Oughaddou, H. Enriquez, A. Kara, S. Vizzini, B. Ealet, and B. Aufray, Appl. Phys. Lett. **97**, 223109 (2010).
[15] B. Aufray, A. Kara, S. Vizzini, H. Oughaddou, C. Leandri, B. Ealet, and G. Le Lay, Appl. Phys. Lett. **96**, 183102 (2010).
[16] D. Jose and A. Datta, Acc. Chem. Res. **47**, 593 (2013).
[17] A. Nijamudheen, R. Bhattacharjee, S. Choudhury, and A. Datta, J. Phys. Chem. C **119**, 3802 (2015).
[18] Z. Ni, H. Zhong, X. Jiang, R. Quhe, G. Luo, Y. Wang, M. Ye, J. Yang, J. Shi, and J. Lu, Nanoscale **6**, 7609 (2014).
[19] Y. Du, J. Zhuang, H. Liu, X. Xu, S. Eilers, K. Wu, P. Cheng, J. Zhao, X. Pi, K. W. See *et al.*, ACS Nano **8**, 10019 (2014).
[20] L. E. Gusel'Nikov and N. S. Nametkin, Chem. Rev. **79**, 529 (1979).
[21] P. Jutzi, Angew. Chem. Int. Ed. **14**, 232 (1975).
[22] R. S. Mulliken, J. Am. Chem. Soc. **72**, 4493 (1950).
[23] J. C. Garcia, D. B. de Lima, L. V. C. Assali, and J. F. Justo, J. Phys. Chem. C **115**, 13242 (2011).
[24] H. Liu, A. T. Neal, Z. Zhu, Z. Luo, X. Xu, D. Tománek, and P. D. Ye, ACS Nano **8**, 4033 (2014).
[25] A. Castellanos-Gómez, L. Vicarelli, E. Prada, J. O. Island, K. L. Narasimha-Acharya, S. I. Blanter, D. J. Groenendijk, M. Buscema, G. A. Steele, J. V. Alvarez *et al.*, 2D Mater. **1**, 025001 (2014).
[26] F. Xia, H. Wang, and Y. Jia, Nat. Commun. **5**, 4458 (2014).
[27] J. D. Wood, S. A. Wells, D. Jariwala, K.-S. Chen, E. Cho, V. K. Sangwan, X. Liu, L. J. Lauhon, T. J. Marks, and M. C. Hersam, Nano Lett. **14**, 6964 (2014).

[28] J. O. Island, G. A. Steele, H. S. J. van der Zant, and A. Castellanos-Gómez, 2D Mater. **2**, 011002 (2015).
[29] L. Li, Y. Yu, G. J. Ye, Q. Ge, X. Ou, H. Wu, D. Feng, X. H. Chen, and Y. Zhang, Nat. Nanotechnol. **9**, 372 (2014).
[30] A. Castellanos-Gómez, J. Phys. Chem. Lett. **6**, 4280 (2015).
[31] C. Kamal and M. Ezawa, Phys. Rev. B **91**, 085423 (2015).
[32] S. Zhang, Z. Yan, Y. Li, Z. Chen, and H. Zeng, Angew. Chem. Int. Ed. **54**, 3112 (2015).
[33] W. Yu, C.-Y. Niu, Z. Zhu, X. Wang, and W.-B. Zhang, J. Mater. Chem. C **4**, 6581 (2016).
[34] L. C. Gomes, A. Carvalho, and A. H. Castro Neto, Phys. Rev. B **92**, 214103 (2015).
[35] B. R. Tuttle, S. M. Alhassan, and S. T. Pantelides, Phys. Rev. B **92**, 235405 (2015).
[36] M. Mehboudi, A. M. Dorio, W. Zhu, A. van der Zande, H. O. H. Churchill, A. A. Pacheco-Sanjuan, E. O. Harriss, P. Kumar, and S. Barraza-Lopez, Nano Lett. **16**, 1704 (2016).
[37] A. K. Singh and R. G. Hennig, Appl. Phys. Lett. **105**, 042103 (2014).
[38] Z. Zhu, J. Guan, D. Liu, and D. Tománek, ACS Nano **9**, 8284 (2015).
[39] S. Karmakar, C. Chowdhury, and A. Datta, J. Phys. Chem. C **120**, 14522 (2016).
[40] A. Ayuela, J. S. Dolado, I. Campillo, Y. R. De Miguel, E. Erkizia, D. Sánchez-Portal, A. Rubio, A. Porro, and P. M. Echenique, J. Chem. Phys **127**, 164710 (2007).
[41] H. Kwart and K. King, *d-Orbitals in the Chemistry of Silicon, Phosphorus and Sulfur*, Vol. 3 (Springer Science, Berlin, Heildelberg, 1997).
[42] J. P. Perdew, K. Burke, and M. Ernzerhof, Phys. Rev. Lett. **77**, 3865 (1996).
[43] N. Troullier and J. L. Martins, Phys. Rev. B **43**, 1993 (1991).
[44] A. M. Souza, A. R. Rocha, A. Fazzio, and A. J. R. da Silva, AIP Adv. **2**, 032115 (2012).
[45] Z. Zanolli and J.-C. Charlier, Phys. Rev. B **80**, 155447 (2009).
[46] E. Hobi Jr., R. B. Pontes, A. Fazzio, and A. J. R. da Silva, Phys. Rev. B **81**, 201406 (2010).
[47] P. E. Blöchl, Phys. Rev. B **50**, 17953 (1994).
[48] G. Kresse and D. Joubert, Phys. Rev. B **59**, 1758 (1999).
[49] J.-H. Yang, Y. Zhang, W.-J. Yin, X. Gong, B. I. Yakobson, and S.-H. Wei, Nano Lett. **16**, 1110 (2016).
[50] See Supplemental Material at http://link.aps.org/supplemental/10.1103/PhysRevB.94.245441 for animation of molecular dynamics, analysis of the electronic structure of alpha and beta SiS monolayers, and two more SiS metastable nanostructures.
[51] J. Guan, Z. Zhu, and D. Tománek, Phys. Rev. Lett. **113**, 046804 (2014).
[52] H. E. Bergna and W. O. Roberts, *Colloidal Silica: Fundamentals and Applications*, Vol. 131 (CRC Press, Boca Raton, FL, 2005).
[53] S. Cahangirov, V. O. Özçelik, L. Xian, J. Avila, S. Cho, M. C. Asensio, S. Ciraci, and A. Rubio, Phys. Rev. B **90**, 035448 (2014).
[54] Consideration of the charge transfer under the Mulliken scheme represents another step towards further understanding of the electronic structure of the γ phase of silicon monosulfide. As expected due to the larger electronegativity of sulfur with respect to that of silicon, 0.4 electrons pass from the silicon to the sulfur atom. For α and β, we find values of 0.46 and 0.33 electrons, respectively, which are slightly higher than those given by Zhu *et al.* [38], of 0.3 and 0.2 electrons, respectively. It appears that for the three monolayers, both the trend and the amount of charge transfer are similar. Considering the SiS phases, the charge transfers do not present noticeable differences that can explain the gain in stability. Consequently, a different approach is required to identify the reason behind the enhanced binding energy per atom such as the extra Si-Si bond producing *spd* hybridization in silicon.